AMERICAN SOCIETY FOR MICROBIOLOGY | mBio®

RESEARCH ARTICLE

Interferon Lambda Signals in Maternal Tissues to Exert Protective and Pathogenic Effects in a Gestational Stage-Dependent Manner

Rebecca L. Casazza,[a] Drake T. Philip,[a] Helen M. Lazear[a]

[a]Department of Microbiology and Immunology, University of North Carolina at Chapel Hill, Chapel Hill, North Carolina, USA

ABSTRACT Interferon lambda (IFN-λ) (type III IFN) is constitutively secreted from human placental cells in culture and reduces Zika virus (ZIKV) transplacental transmission in mice. However, the roles of IFN-λ during healthy pregnancy and in restricting congenital infection remain unclear. Here, we used mice lacking the IFN-λ receptor (*Ifnlr1*$^{-/-}$) to generate pregnancies lacking either maternal or fetal IFN-λ responsiveness and found that the antiviral effect of IFN-λ resulted from signaling exclusively in maternal tissues. This protective effect depended on gestational stage, as infection earlier in pregnancy (E7 rather than E9) resulted in enhanced transplacental transmission of ZIKV. In *Ifnar1*$^{-/-}$ dams, which sustain robust ZIKV infection, maternal IFN-λ signaling caused fetal resorption and intrauterine growth restriction. Pregnancy pathology elicited by poly(I·C) treatment also was mediated by maternal IFN-λ signaling, specifically in maternal leukocytes, and also occurred in a gestational stage-dependent manner. These findings identify an unexpected effect of IFN-λ signaling, specifically in maternal (rather than placental or fetal) tissues, which is distinct from the pathogenic effects of IFN-$\alpha\beta$ (type I IFN) during pregnancy. These results highlight the complexity of immune signaling at the maternal-fetal interface, where disparate outcomes can result from signaling at different gestational stages.

IMPORTANCE Pregnancy is an immunologically complex situation, which must balance protecting the fetus from maternal pathogens with preventing maternal immune rejection of non-self fetal and placental tissue. Cytokines, such as interferon lambda (IFN-λ), contribute to antiviral immunity at the maternal-fetal interface. We found in a mouse model of congenital Zika virus infection that IFN-λ can have either a protective antiviral effect or cause immune-mediated pathology, depending on the stage of gestation when IFN-λ signaling occurs. Remarkably, both the protective and pathogenic effects of IFN-λ occurred through signaling exclusively in maternal immune cells rather than in fetal or placental tissues or in other maternal cell types, identifying a new role for IFN-λ at the maternal-fetal interface.

KEYWORDS IFN, IFN-λ, interferon, Zika virus, congenital infection, pregnancy

Immune regulation at the maternal-fetal interface is complex due to conflicting immunological objectives: protection of the fetus from maternal pathogens and prevention of immune-mediated rejection of the semi-allogeneic fetus and placenta. The few pathogens able to surmount the placental barrier and cause congenital infections include Zika virus (ZIKV), rubella virus (RUBV), and human cytomegalovirus (HCMV) (1). The mechanisms by which pathogens are excluded from the fetal compartment are not fully understood, and it is unclear how antiviral activity at the maternal-fetal interface affects tolerogenic immunity. Moreover, pregnancy encompasses multiple developmental stages, including implantation, fetal growth, and parturition, each with unique immunologic requirements (2–4). Because the physiology and immunology of

Editor Thomas E. Morrison, University of Colorado School of Medicine

Address correspondence to Helen M. Lazear, helen.lazear@med.unc.edu.

The authors declare no conflict of interest.

Received 29 December 2021
Accepted 28 March 2022

the placenta change over gestation, there likely are distinct antiviral mechanisms at each stage of pregnancy.

The need to balance protective and pathogenic immunity is not unique to the maternal-fetal interface: epithelial surfaces such as the gastrointestinal and respiratory tracts encounter microbes and must provide protection from pathogens without inflicting inflammatory damage. Interferon lambda (IFN-λ) (type III IFN) is a cytokine that elicits a similar antiviral transcriptional response as type I IFNs (IFN-αβ) but signals through a distinct heterodimeric receptor comprised of IFNLR1 and IL10Rb. (5). The IFN-λ receptor is predominantly expressed on epithelial cells and consequently confers antiviral protection at barrier surfaces including the gastrointestinal and respiratory tracts. IFN-λ is secreted constitutively from human midgestation and term placental explants and trophoblasts cultured *ex vivo*, human trophoblast organoids, and human placental cell lines syncytialized in culture (6–8). In a mouse model of congenital ZIKV infection, IFN-λ restricted transplacental transmission, as fetuses from *Ifnlr1*$^{-/-}$ pregnancies (*Ifnlr1*$^{-/-}$ × *Ifnlr1*$^{-/-}$) sustained higher fetal and placental viral loads than those from wild-type (WT) pregnancies (9). However, the mechanism by which IFN-λ protects against viral infection at the maternal-fetal interface has not been defined.

The 2015 to 2017 ZIKV outbreak throughout Latin America and the Caribbean revealed that ZIKV infection during pregnancy can produce a spectrum of adverse fetal and neonatal outcomes (collectively referred to as congenital Zika syndrome), including microcephaly, intrauterine growth restriction (IUGR), placental insufficiency, vision and hearing loss, as well as miscarriage and stillbirth (10, 11). Infants born without overt congenital Zika syndrome also can have cognitive or functional deficits that become evident later in infancy or childhood (12–14). Mouse models of ZIKV congenital infection have been developed to test vaccines and antivirals as well as to define ZIKV pathogenic mechanisms and antiviral immunity at the maternal-fetal interface (15–17). Aspects of ZIKV fetal pathogenesis are recapitulated in mouse models and include fetal loss, IUGR, fetal brain infection, placental pathology, and neurologic defects. The outcomes of congenital ZIKV infection usually are more severe when infection occurs earlier in gestation in both mice (9, 15, 18) and humans (19–22). Although there are differences between mouse and human pregnancy (23), mice provide a genetically tractable system to study antiviral and placental immunity at distinct gestational time points.

Here, we used mouse models of congenital ZIKV infection to determine the targets of IFN-λ signaling by infecting pregnancies that lacked IFN-λ signaling (*Ifnlr1*$^{-/-}$) in maternal and/or fetal tissues. When we infected at embryonic day 9 (E9), we observed that IFN-λ signaling in maternal tissues protected against transplacental ZIKV transmission. Surprisingly, IFN-λ had a deleterious effect when pregnancies were infected 2 days earlier at E7, with IFN-λ responsive dams exhibiting higher rates of ZIKV transmission as well as overt pathology and fetal resorption. This effect was not specific to ZIKV, as we also found that maternal IFN-λ signaling increased rates of fetal loss after poly(I·C) treatment and that this pathology similarly was dependent on gestational age at the time of administration. These findings identify an unexpected effect of IFN-λ signaling specifically in maternal (rather than placental or fetal) tissues and highlight the complexity of immune signaling at the maternal-fetal interface, where disparate outcomes can result from signaling at different gestational stages.

RESULTS

ZIKV congenital infection is exacerbated earlier in pregnancy and in *Ifnar1*$^{-/-}$ dams. ZIKV replication in mice is restricted by the IFN response because ZIKV is unable to antagonize mouse STAT2 (24, 25). Thus, mouse models of ZIKV pathogenesis typically employ mice lacking IFN-αβ signaling, usually through genetic loss of the IFN-αβ receptor (*Ifnar1*$^{-/-}$) alone or in combination with the IFN-γ receptor (*Ifnar1*$^{-/-}$ *Ifngr1*$^{-/-}$ double knockout (DKO), or by treatment of wild-type mice with an IFNAR1-blocking monoclonal antibody (MAR1-5A3) (26). Congenital ZIKV pathogenesis has been studied in many

different mouse models that vary in mouse genetic background, IFN responsiveness, ZIKV strain, inoculation route, duration of infection, and gestational stage at infection and harvest (27). To better define the conditions that produce transplacental transmission and pathology, we evaluated gross pathology and fetal viral loads in pregnant *Ifnar1*$^{-/-}$ dams or wild-type dams treated with 2 mg of MAR1-5A3 1 day prior to infection. To exclude fetal pathology resulting from severe maternal morbidity, we first compared the virulence of three Asian-lineage ZIKV strains in nonpregnant female 8- to 10-week-old *Ifnar1*$^{-/-}$ mice infected with 1,000 focus-forming units (FFU) of ZIKV by subcutaneous inoculation in the footpad (Fig. 1A and B). We found that strain H/PF/2013 was the most virulent, causing 80% lethality, whereas strain FSS13025 caused modest weight loss in some mice and only 20% lethality, and strain PRVABC59 caused no weight loss or lethality, altogether consistent with prior studies reporting the relative virulence of these strains in *Ifnar1*$^{-/-}$ mice of various ages and inoculation routes (25, 26, 28). We chose to use strain FSS13025 for further experiments to achieve robust maternal infection without severe maternal morbidity and because of its use in studies from other groups evaluating the role of IFN signaling in congenital ZIKV infection (29). We infected pregnant dams with 1,000 FFU of ZIKV FSS13025 by subcutaneous inoculation in the footpad at E7 or E9 (Fig. 1C) and measured viral loads in the maternal spleen, placentas, and fetal heads at E15 (8 or 6 days postinfection [dpi]) by reverse-transcription quantitative PCR (qRT-PCR), (Fig. 1D to F). We chose E7 and E9 for comparison because both represent infection early in pregnancy but are expected to allow the infection to reach the maternal-fetal interface either before (E7 infection) or after (E9 infection) formation of the placental barrier at E10.5 and are within the gestational window within which others observe pathological differences in congenital ZIKV infection (9, 30, 31). We observed higher viral loads in *Ifnar1*$^{-/-}$ dams than in WT dams treated with MAR1-5A3, and viral loads were higher after infection at E9 (6 dpi) than infection at E7 (8 dpi). Placental and fetal viral loads corresponded to maternal spleen viral loads, suggesting that fetal infection increases with the severity of maternal infection. Rates of transplacental transmission (measured by proportion of fetal heads that were ZIKV positive) were higher in *Ifnar1*$^{-/-}$ dams than MAR1-5A3-treated dams (64% versus 57% at E7 and 100% versus 61% at E9). All fetuses that were intact (not resorbed) were photographed and weighed (Fig. 1G to I). Fetuses smaller than one standard deviation below the mean of uninfected pregnancies were classified as having IUGR. *Ifnar1*$^{-/-}$ dams exhibited significantly higher resorption rates than uninfected controls. In contrast to fetal viral loads, which were higher in dams infected at E9, fetal pathology was greater in dams infected at E7, suggesting higher placental/fetal susceptibility early in pregnancy or that pathology increases with longer infection times. The results were the same when we assessed pathology by crown-rump length (CRL) rather than fetal weight (see Fig. S1A and B in the supplemental material). These results indicate that there are significant differences in adverse pregnancy outcomes when infections occur at different gestational stages and that fetal pathological outcomes and viral loads are more severe in the context of high maternal infection (*Ifnar1*$^{-/-}$).

To determine if we could observe similar pregnancy pathology with another virus that causes congenital infections in humans, we sought to generate a RUBV mouse model, as small animal models to study RUBV pathogenesis are not available and experimental RUBV infections in knockout mice have not been reported. We first infected 8-week-old nonpregnant wild-type, *Ifnar1*$^{-/-}$, and *Ifnlr1*$^{-/-}$ mice with 1,000 FFU and 5-week-old *Ifnar1*$^{-/-}$ mice with 1×10^5 FFU of RUBV (strain M33) by intranasal inoculation or subcutaneous inoculation in the footpad but observed no weight loss or disease signs (see Fig. S2A and B in the supplemental material). To determine whether mice supported any RUBV infection, we inoculated *Ifnar1*$^{-/-}$ *Ifngr1*$^{-/-}$ DKO mice intravenously with 1×10^5 FFU of RUBV and measured viral RNA by (qRT-PCR) from blood and serum at 2, 4, and 7 dpi and from spleen, lung, and kidney at 7 dpi (Fig. S2C and D). Although in humans RUBV targets a variety of tissues and produces viremia (32), we found very low or undetectable viral loads in *Ifnar1*$^{-/-}$ *Ifngr1*$^{-/-}$ DKO mice, even though these mice are highly susceptible to many viral infections. Since human

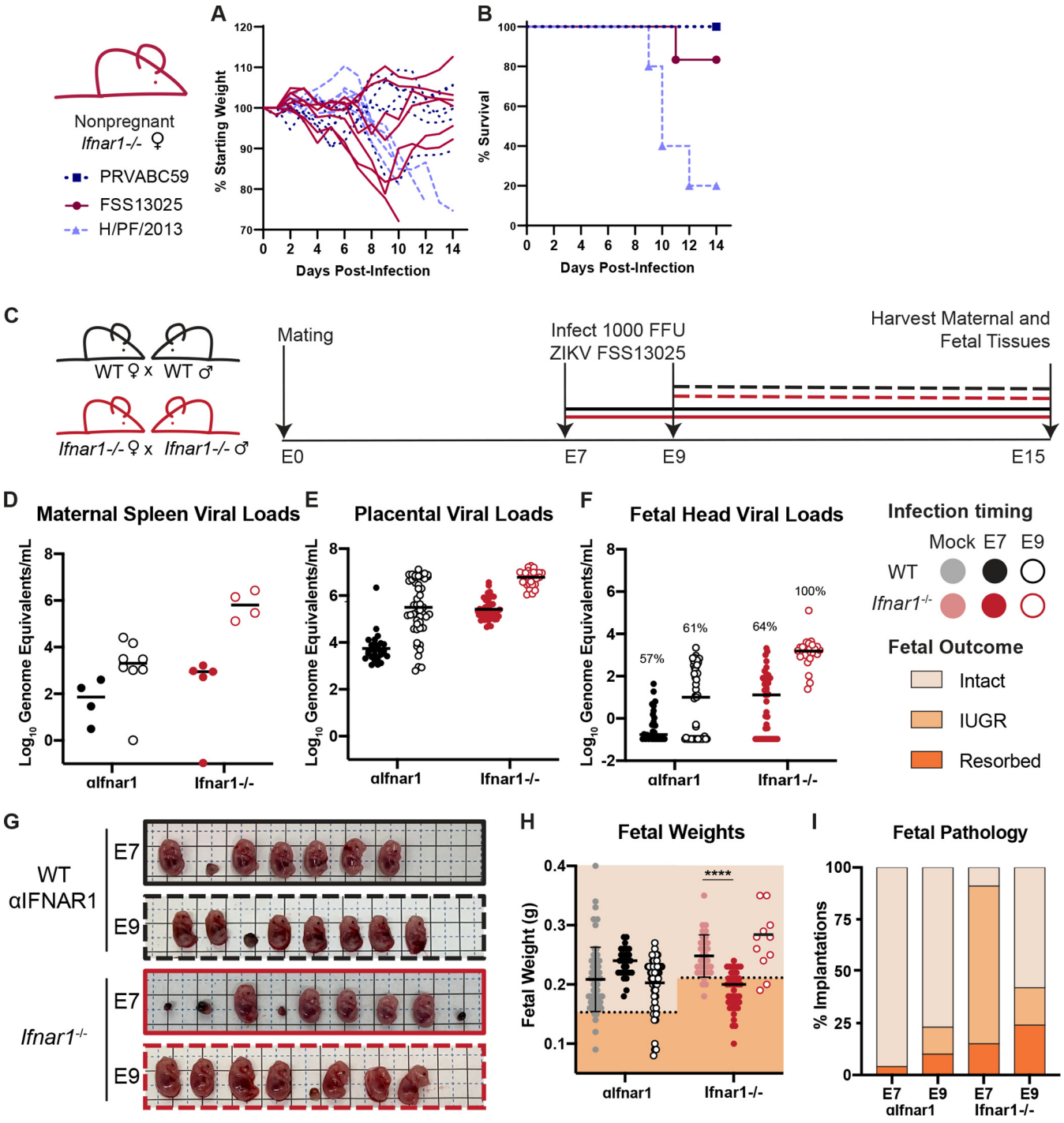

FIG 1 Infection earlier in gestation corresponds to enhanced fetal pathology in mouse models of congenital ZIKV infection. (A and B) Nonpregnant 8- to 10-week-old female *Ifnar1*$^{-/-}$ mice (5 to 6 mice per group) were infected with 1,000 FFU of ZIKV strain PRVABC59, FSS13025, or H/PF/2013; weights and survival were measured daily for 14 days. Each line in (A) represents an individual mouse. (C) Dams from WT × WT or *Ifnar1*$^{-/-}$ × *Ifnar1*$^{-/-}$ crosses (6 to 8 WT or 4 to 5 *Ifnar1*$^{-/-}$ dams per group) were infected at day 7 or 9 postmating (E7, E9) with ZIKV FSS13025 by subcutaneous inoculation in the footpad. WT dams were given 2 mg of anti-IFNAR1 blocking monoclonal antibody (MAb) intraperitoneally 1 day prior to infection. Tissues were harvested at E15 (8 or 6 dpi). (D to F) ZIKV viral loads in the maternal spleen, placenta, and fetal head were measured by qRT-PCR. Each data point represents one dam (D) or fetus (E and F). The percent of ZIKV-positive fetal heads is indicated above each group. (G) Representative images of fetuses/resorptions from one pregnancy from each cross. (H) Intact fetuses (i.e., not resorbed) were weighed. Fetuses <1 standard deviation from the mean of mock-infected (below dotted line) were classified as having intrauterine growth restriction (IUGR). Intact fetuses with weights significantly different from mock pregnancies (calculated by ANOVA) are indicated; ****, $P < 0.0001$. (I) Proportions of fetuses exhibiting IUGR or resorption.

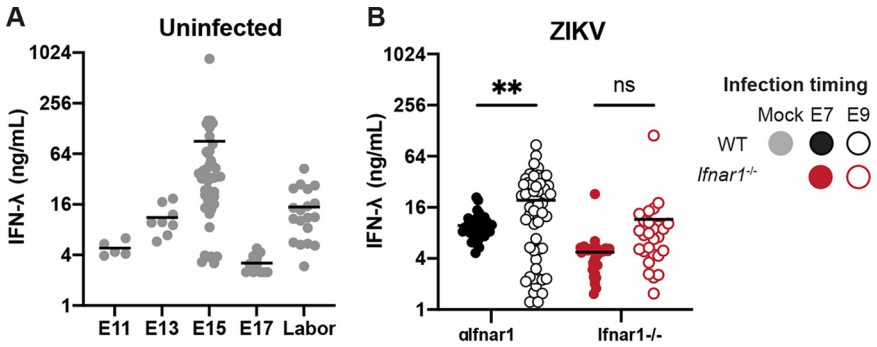

FIG 2 IFN-λ is produced at the maternal-fetal interface. (A) Placentas were harvested from uninfected pregnant dams at E11 (1 dam), E13 (1 dam), E15 (5 dams), E17 (3 dams), and during labor (3 dams). Placentas were homogenized in PBS, and IFN-λ activity in placental homogenate was determined using a reporter cell line. (B) Pregnant WT dams (treated with an anti-IFNAR1 blocking MAb, 6 or 8 dams per group) or pregnant *Ifnar1*$^{-/-}$ dams (4 or 5 dams per group) were infected at either E7 or E9 with ZIKV FSS13025. Placentas were homogenized in PBS, and IFN-λ activity in placental homogenate was determined using a reporter cell line.

congenital rubella syndrome requires maternal viremia, we concluded that this mouse model would not be suitable for assessing transplacental transmission of RUBV and limited our further studies to ZIKV.

Midgestation mouse placentas produce IFN-λ in the presence and absence of infection. IFN-λ is secreted constitutively from human primary trophoblasts cultured *ex vivo*, trophoblast organoids, and placental cell lines grown in three-dimensional (3D) culture (6–8). Although IFN-λ has antiviral activity at the murine maternal-fetal interface (9), it was unknown if IFN-λ was secreted constitutively from the mouse placenta. To evaluate IFN-λ activity in the absence of infection, we measured IFN-λ activity from placentas harvested from mid-to-late gestation (E11 to labor). In uninfected mice, we found that placental IFN-λ activity varied considerably over the course of gestation, increasing from E11 to E15 and then dropping at E17 (Fig. 2A). IFN-λ activity rose again in placentas taken from dams in active labor, consistent with the cytokine response that triggers parturition. We also detected IFN-λ in the placentas of ZIKV-infected dams harvested at E15 (Fig. 2B). Placentas from MAR1-5A3-treated WT dams infected at E9 had significantly higher IFN-λ activity than placentas from dams infected at E7, but there was no effect of infection timing in *Ifnar1*$^{-/-}$ dams. These results indicate that IFN-λ is constitutively expressed during mouse pregnancy and also is present during congenital ZIKV infection.

Maternal IFN-λ signaling restricts ZIKV transplacental transmission in a gestational stage-dependent manner. Prior studies found that IFN-λ signaling reduces ZIKV transplacental transmission in mice (9), but the cells and tissues responding to IFN-λ were not identified. To determine the targets of IFN-λ signaling at the maternal-fetal interface, we first assessed whether the protective effects of IFN-λ were mediated by signaling in maternal or fetal tissues. To generate pregnancies with distinct maternal and fetal IFN-λ responsiveness, we crossed *Ifnlr1*$^{+/-}$ dams and *Ifnlr1*$^{-/-}$ sires, or the reverse, producing litters comprising *Ifnlr1*$^{+/-}$ and *Ifnlr1*$^{-/-}$ fetuses within dams that either retained IFN-λ signaling (*Ifnlr1*$^{+/-}$) or lacked it (*Ifnlr1*$^{-/-}$) (Fig. 3A). We infected mice with 1,000 FFU of ZIKV FSS13025 by subcutaneous inoculation in the footpad at E9, 1 day following administration of 2 mg of MAR1-5A3. At 6 dpi (E15), we harvested maternal and fetal tissues and determined fetal *Ifnlr1* genotype by PCR and viral loads by qRT-PCR. We found no difference in maternal or placental viral loads based on maternal or fetal *Ifnlr1* genotype (Fig. 3B and C). In contrast, we found higher rates of ZIKV transplacental transmission in dams lacking IFN-λ signaling (*Ifnlr1*$^{-/-}$), regardless of fetal genotype (67% versus 28%), and viral loads were significantly higher in fetuses from *Ifnlr1*$^{-/-}$ dams compared to those from *Ifnlr1*$^{+/-}$ dams, regardless of fetal genotype ($P < 0.0001$) (Fig. 3D). Higher viral loads were not accompanied by overt pathology in this model, as there was no difference in fetal weights (Fig. 3E) based on either

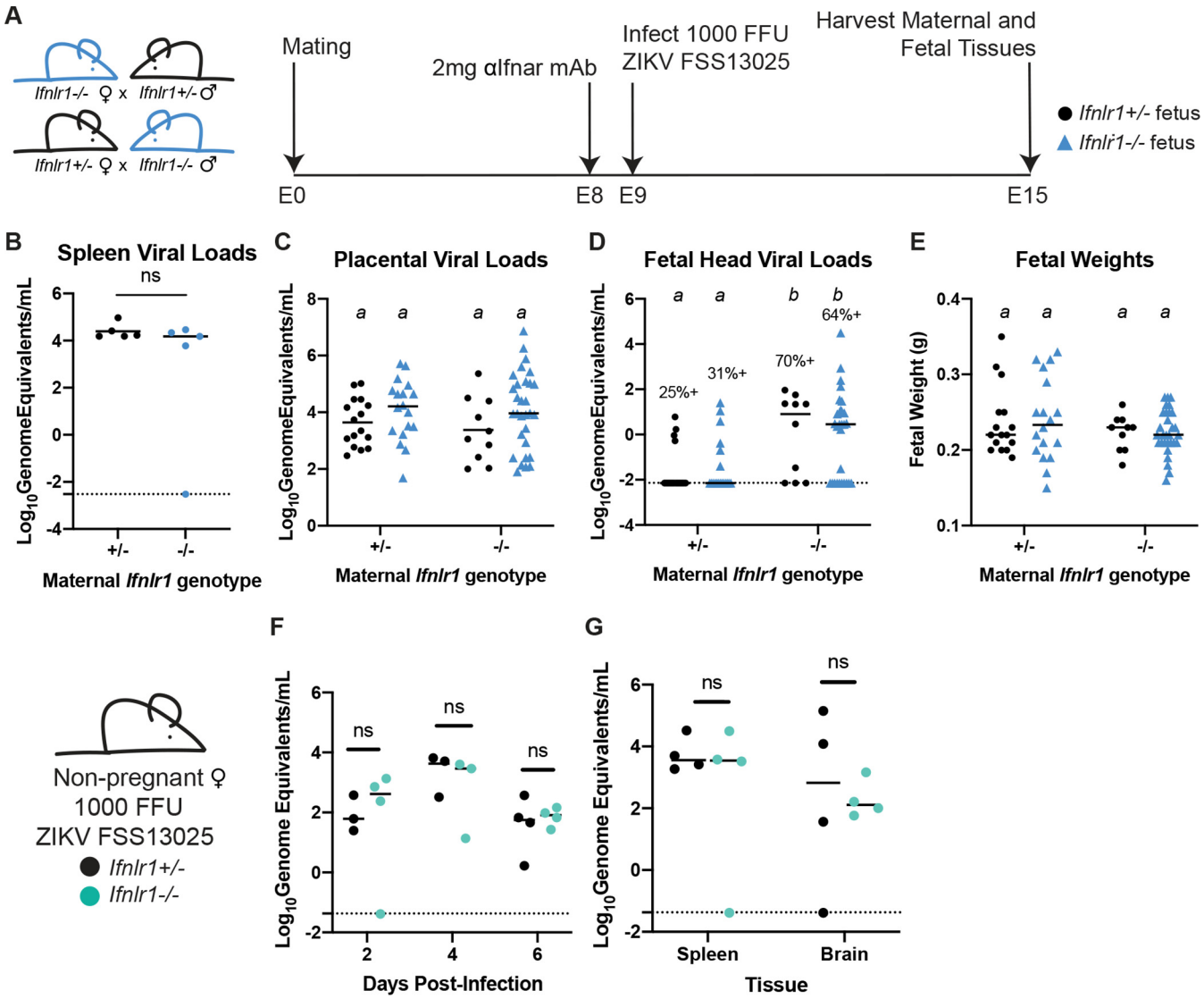

FIG 3 IFN-λ restricts ZIKV transplacental transmission by signaling to maternal tissues. (A) Mating and infection timeline. *Ifnlr1*$^{+/-}$ dam × *Ifnlr1*$^{-/-}$ sire and *Ifnlr1*$^{-/-}$ dam × *Ifnlr1*$^{+/-}$ sire crosses were used to generate pregnancies with IFN-λ responsive (*Ifnlr1*$^{+/-}$) and nonresponsive (*Ifnlr1*$^{-/-}$) fetuses. (B to E) Pregnant dams were treated with 2 mg of IFNAR1 blocking antibody at E8 and infected at E9 with 1,000 FFU of ZIKV FSS13025 by subcutaneous inoculation in the footpad. Fetuses and their associated placentas were harvested at E15. ZIKV RNA was measured by qRT-PCR in maternal spleen (B), placenta (C), and fetal head (D), and fetuses were weighed (E). (D) The percent of fetuses with detectable ZIKV is noted. Data are combined from 5 or 6 dams per group; each data point represents a single dam (B) or fetus (C to E). Groups were compared by ANOVA (B, C, E) or Mann-Whitney (D); italicized letters indicate groups that are significantly different from each other ($P < 0.05$). (F and G) Nonpregnant, 8-week-old *Ifnlr1*$^{-/-}$ and *Ifnlr1*$^{+/-}$ females were infected with 1,000 FFU of ZIKV FSS13025. Viremia was measured from serum at 2, 4, and 6 dpi by qRT-PCR. Spleens and brains were harvested 6 dpi, and viral loads were measured by qRT-PCR. Groups were not significantly different (ns) by ANOVA.

maternal or fetal *Ifnlr1* genotype. Our observation of higher viral loads in the fetuses of *Ifnlr1*$^{-/-}$ dams, regardless of fetal *Ifnlr1* genotype, provides strong evidence that IFN-λ signaling protects against transplacental transmission of ZIKV via signaling exclusively in maternal tissues. This is specific to tissues at the maternal fetal-interface, as nonpregnant female *Ifnlr1*$^{-/-}$ and *Ifnlr1*$^{+/-}$ mice exhibited no differences in viremia or tissue viral loads following infection (Fig. 3F and G).

In mice, placental differentiation is complete around E10.5 (30), so mice infected at E9 are expected to have a fully formed placenta by the time ZIKV reaches the placenta from maternal circulation. Since pregnancy pathology depends on gestational stage at the time of infection (Fig. 1) (9, 29) and IFN-λ antiviral effects vary with gestational time (9), we next assessed the effects of IFN-λ signaling in maternal and fetal tissues following ZIKV infection 2 days earlier, at E7. At this earlier infection time,

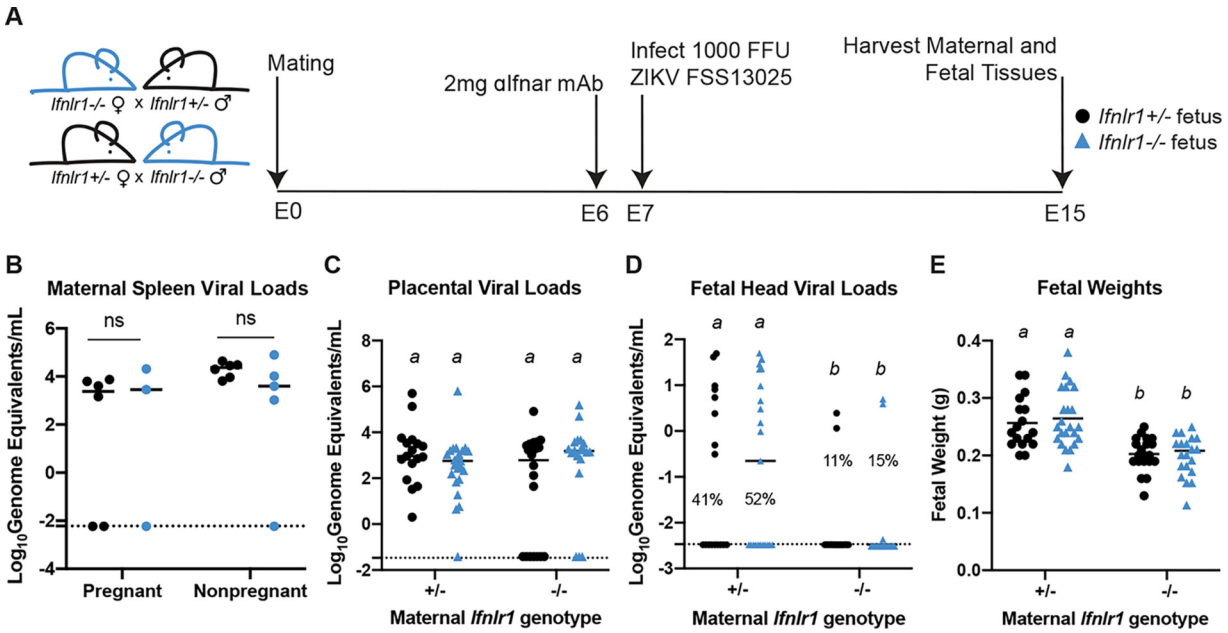

FIG 4 IFN-λ enhances fetal infection early in gestation through signaling to maternal tissues. (A) Mating and infection timeline. *Ifnlr1*$^{+/-}$ dam × *Ifnlr1*$^{-/-}$ sire and *Ifnlr1*$^{-/-}$ dam × *Ifnlr1*$^{+/-}$ sire crosses were treated with 2 mg of anti-IFNAR1 MAb at E6 and infected at E7 with 1,000 FFU of ZIKV FSS13025 by subcutaneous inoculation in the footpad. Fetuses and their associated placentas were harvested at E15. (B to D) ZIKV RNA in the maternal spleens, placenta, and fetal head were measured by qRT-PCR. (E) Gross fetal pathology was measured by fetal weight. Groups were compared by ANOVA (B, C, E) or Mann-Whitney (D); italicized letters indicate groups that are significantly different from each other ($P < 0.05$). Data are combined from 5 or 6 dams per group; each data point represents a single dam (B) or fetus (C to E).

maternal viremia is expected to be established prior to complete placentation. We again crossed *Ifnlr1*$^{+/-}$ and *Ifnlr1*$^{-/-}$ mice to generate pregnancies with mixed IFN-λ responsiveness within dams that could or could not respond to IFN-λ (Fig. 4A). We infected pregnant dams with 1,000 FFU of ZIKV FSS13025 by subcutaneous inoculation in the footpad at E7, 1 day following administration of 2 mg of MAR1-5A3. At 8 dpi (E15), we harvested maternal and fetal tissues and determined *Ifnlr1* genotype by PCR and viral loads by qRT-PCR. Similar to infection at E9, we found no difference in maternal spleen or placental viral load in *Ifnlr1*$^{-/-}$ compared to *Ifnlr1*$^{+/-}$ dams (Fig. 4B and C). However, in contrast to the protective effect of maternal IFN-λ signaling after E9 infection, with E7 infection, we found higher rates of transplacental transmission in *Ifnlr1*$^{+/-}$ dams compared to those of *Ifnlr1*$^{-/-}$ (47% versus 13%; $P = 0.0006$) (Fig. 4D). Moreover, fetuses from *Ifnlr1*$^{+/-}$ dams had significantly higher viral burdens than those from *Ifnlr1*$^{-/-}$ dams, regardless of fetal genotype (Fig. 4D). Although we found significant differences in fetal weights from *Ifnlr1*$^{+/-}$ and *Ifnlr1*$^{-/-}$ dams ($P < 0.0001$), the difference results from an increase in fetal weights from *Ifnlr1*$^{+/-}$ pregnancies, and *Ifnlr1*$^{-/-}$ fetal weights fell within the range of uninfected pregnancies (Fig. 1H and I). Altogether, these results show that IFN-λ signaling exerts a gestational stage-specific effect on ZIKV transplacental transmission, where earlier in gestation IFN-λ signaling facilitates ZIKV transplacental transmission in contrast to later stages where IFN-λ inhibits transplacental transmission. Importantly, at either stage, the effects of IFN-λ signaling were mediated through signaling in maternal tissues rather than through signaling in the placenta or fetus, as only maternal *Ifnlr1* genotype influenced ZIKV transmission, not fetal *Ifnlr1* genotype.

Maternal IFN-λ signaling exacerbates fetal pathology early in gestation. Since maternal IFN-λ signaling enhanced rather than limited ZIKV transmission at E7, we next assessed the effects of IFN-λ signaling on fetal pathology at this early gestational stage. These experiments used mice that retained or lacked IFN-λ signaling on an *Ifnar1*$^{-/-}$ background, as we did not observe overt pathology in IFNAR1-intact mice (Fig. 1G to I). We crossed wild-type, *Ifnar1*$^{-/-}$, and *Ifnar1*$^{-/-}$ *Ifnlr1*$^{-/-}$ DKO dams and sires to generate pregnancies in which IFN-λ signaling was present or absent on

both or either side of the maternal-fetal interface (Fig. 5A). Pregnant dams were infected with ZIKV FSS13025 at E7, and tissues were harvested 8 dpi (E15). Pregnancies that lacked both IFN-αβ and IFN-λ signaling on both sides of the maternal-fetal interface exhibited significant growth restriction compared to uninfected pregnancies (Fig. 5B to D, group 1). Fetal IFN-αβ signaling previously has been shown to be pathogenic during congenital ZIKV infection in mice (29), and accordingly we found that all fetuses were resorbed in pregnancies that retained IFN-αβ and IFN-λ signaling exclusively on the fetal side of the interface (Fig. 5B to D, group 2). This pathology was mediated by fetal IFN-αβ signaling because when fetal IFN-λ signaling was restored in the absence of fetal IFN-αβ signaling, we found no resorptions (Fig. 5B to D, group 3). In contrast, when IFN-λ signaling was restored on both the fetal and maternal side, 30% of the fetuses were resorbed, and the remaining intact fetuses were significantly smaller than those from uninfected pregnancies (Fig. 5B to D, group 4). Moreover, pregnancies with maternal IFN-λ signaling had variable fetal outcomes (Fig. 5D), both within and between pregnancies (Fig. 5E). There were no significant differences in maternal spleen viral loads or fetal viral load as determined by qRT-PCR (Fig. 5F and G). Since pregnancies with maternal IFN-λ signaling exhibited variable pathological outcomes within litters, we asked whether this was influenced by fetal sex. We determined fetal sex by PCR genotyping for *Sry*, a gene found on the Y chromosome, and found that 40% of male fetuses were resorbed (20% of total implantations) compared to 6% of female fetuses (3% of implantations) (Fig. 5H). This raises the possibility that IFN-λ-mediated outcomes could be driven by maternal immune rejection, as only male fetuses are genetically distinct from the mother in congenic mouse pregnancies. Since our results and prior studies (29) showed that IFN signaling can be pathogenic in the context of congenital ZIKV infection, we considered whether IFN signaling might be detrimental during pregnancy more generally. However, in analyzing ~17 months of breeding records from WT, *Ifnar1*$^{-/-}$, *Ifnlr1*$^{-/-}$, and *Ifnar1*$^{-/-}$ *Ifnlr1*$^{-/-}$ mice in our colony (>275 litters from >40 breeder cages), we found no significant difference in litter size between the lines, supporting the idea that IFN signaling during pregnancy is not detrimental outside an infection or other inflammatory context. We found no difference in viremia or tissue viral loads between *Ifnar1*$^{-/-}$ and *Ifnar1*$^{-/-}$ *Ifnlr1*$^{-/-}$ nonpregnant females (Fig. 5I and J), altogether indicating that the pathogenic effects of IFN-λ at the maternal-fetal interface are distinct from restricting viral replication systemically in the dam.

IFN-λ pathogenic effects are mediated by leukocytes and decrease over gestational time. To determine whether IFN-λ-mediated fetal pathology was specific to ZIKV infection, we assessed the pathogenic effect of IFN-λ signaling stimulated by poly(I·C). To determine which tissues produced IFN in response to poly(I·C) treatment, we measured IFN-λ and IFN-β in serum, uterus, lung, and spleen 24 h post poly(I·C) treatment in pregnant and nonpregnant WT mice. The only tissue in which we detected robust IFN-λ activity (12.7 ng/mL) was the uterus of 1 pregnant dam, while the uterus of another pregnant dam had activity just above the limit of detection (2.8 ng/mL); no IFN-λ activity was detected in the uteruses of nonpregnant mice or in other tissues from pregnant or nonpregnant mice (Fig. 6A). In contrast, IFN-β was detected in uterus, lung, and spleen of pregnant and nonpregnant mice, though not serum (Fig. 6B). These results confirm that poly(I·C) treatment can induce IFN-λ and IFN-αβ at the maternal-fetal interface. We next assessed the effect of poly(I·C) treatment on fetal pathology in *Ifnlr1*$^{+/-}$ and *Ifnlr1*$^{-/-}$ dams mated to WT sires. To investigate the possibility that IFN-λ-mediated pathology resulted from maternal immune signaling, we also included dams lacking IFN-λ signaling in leukocytes (*Vav*-Cre *Ifnlr1*$^{-/-}$) (see Fig. S3 in the supplemental material) mated to WT sires. We administered 200 μg of poly (I·C) by intraperitoneal injection to dams at E7, E9, or E11 and assessed fetal outcome at E15 (Fig. 6C). Consistent with our observations in ZIKV-infected *Ifnar1*$^{-/-}$ dams, *Ifnlr1*$^{+/-}$ dams exhibited a 10-fold higher resorption rate than *Ifnlr1*$^{-/-}$ dams after poly(I·C) administration at E7 (31% versus 3%) (Fig. 6D and E). *Vav*-Cre *Ifnlr1*$^{-/-}$ dams

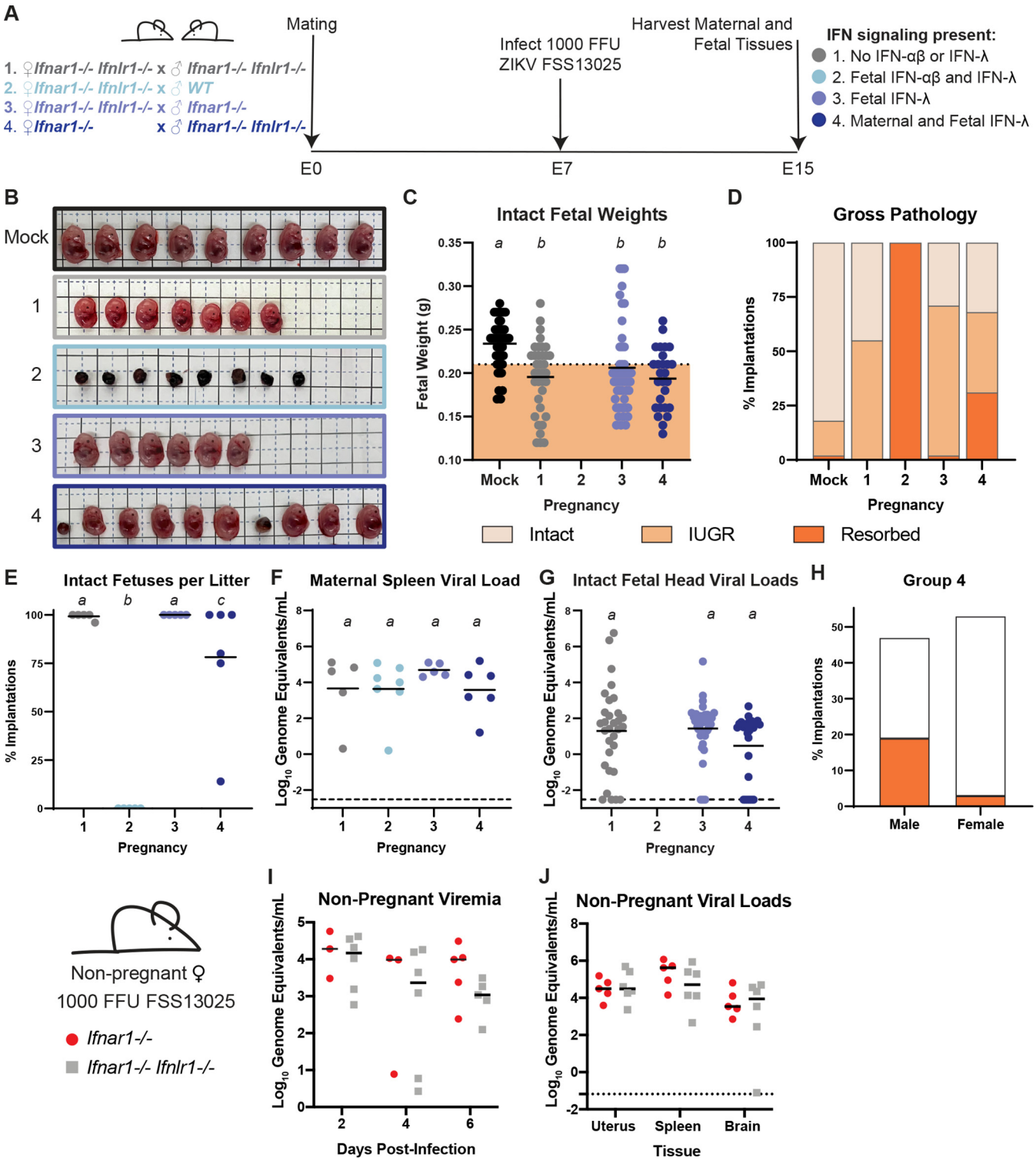

FIG 5 Maternal IFN-λ signaling induces fetal pathology. (A) Mating and infection timeline. Wild-type, *Ifnar1*$^{-/-}$, and *Ifnar1*$^{-/-}$ *Ifnlr1*$^{-/-}$ DKO mice were crossed to create pregnancies with differing IFN-λ responsiveness in maternal and fetal tissues, within dams lacking IFN-αβ signaling. Pregnant dams were infected at E7 with 1,000 FFU of ZIKV FSS13025 by subcutaneous inoculation in the footpad. Data are combined from 5 to 7 dams per group. (B) Representative images of the fetuses/resorptions from each cross. (C) Intact fetuses (not resorbed) were weighed. Fetuses with weights below 1 standard deviation of uninfected pregnancies were classified as having IUGR. Groups were compared by ANOVA; italicized letters indicate groups that are significantly different from each other ($P < 0.05$). (D) The percent of resorptions and IUGR in each pregnancy group. (E) The percent of intact fetuses in individual litters. (F and G) ZIKV viral loads in fetal head and maternal spleen were measured by qRT-PCR. (H) The sex of resorptions and intact fetuses was determined by PCR. (I and J) Ten-week-old nonpregnant females were infected with 1,000 FFU of ZIKV FSS13025 by subcutaneous inoculation in the footpad. Viral loads in serum (2, 4, 6 dpi) and tissues (6 dpi) were determined by qRT-PCR.

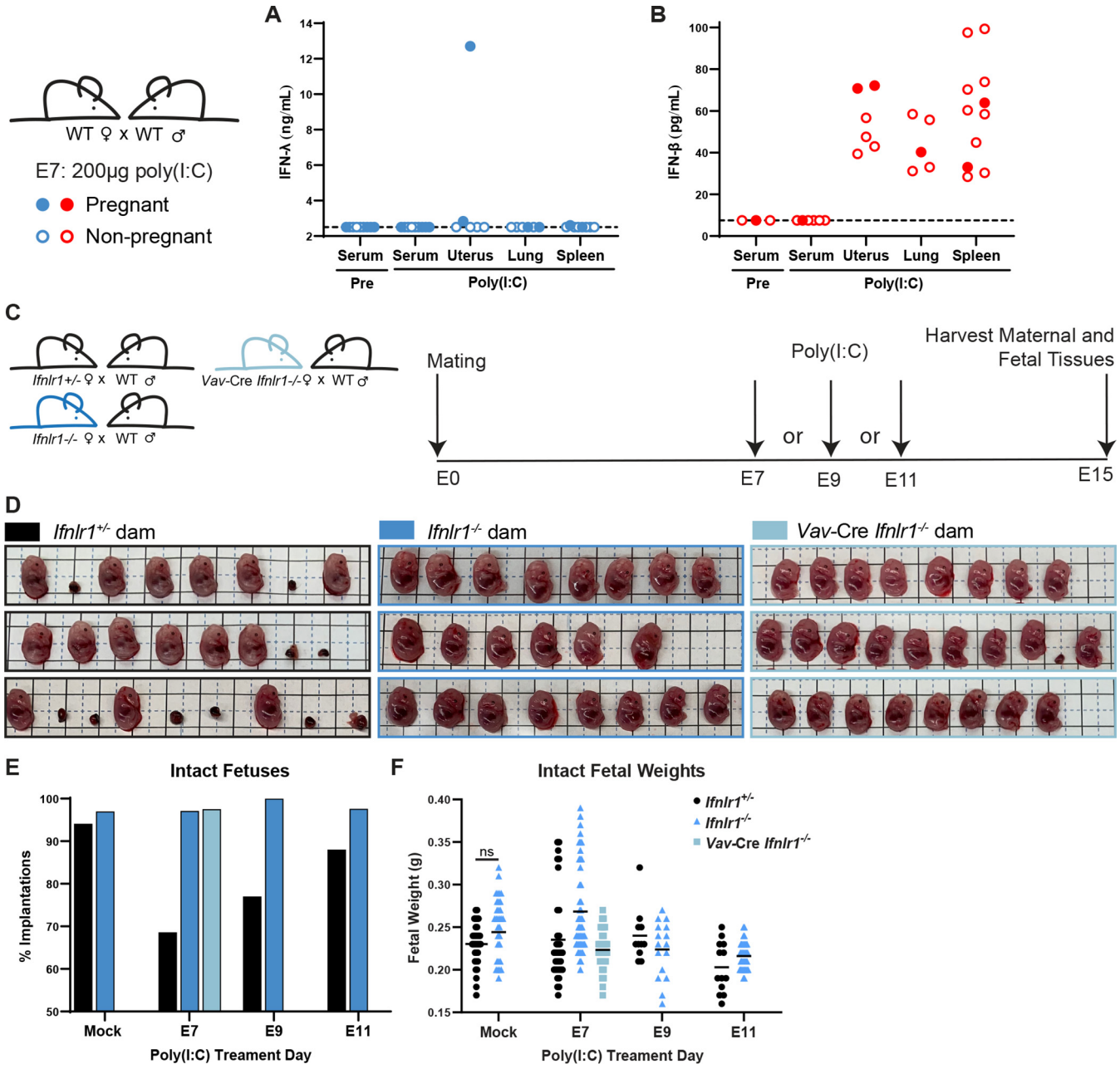

FIG 6 IFN-λ mediates fetal pathology through signaling in maternal leukocytes. (A and B) WT dams were mated to WT sires and treated with 200 μg of poly(I·C) at E7. Serum was collected by submandibular bleed pretreatment. Twenty-four hours posttreatment, serum, uterus, spleen, and lung were harvested from pregnant and nonpregnant mice. IFN-λ activity was measured in a reporter cell assay and IFN-β concentration by ELISA. Filled circles represent pregnant mice. (C) Experiment timeline. *Ifnlr1*$^{+/-}$, *Ifnlr1*$^{-/-}$, and leukocyte *Ifnlr1*$^{-/-}$ (*Vav*-Cre *Ifnlr1*$^{-/-}$) dams were mated to WT sires. Pregnant dams were administered 200 μg of poly(I·C) by intraperitoneal injection at E7, E9, or E11, and fetuses were harvested at E15. Data are combined from 3 to 7 dams per group. (D) Representative litters from E7-treated pregnancies. Resorptions were counted (E) and intact fetuses were weighed (F). Fetal weights were compared by *t* test; no poy(I:C)-treated groups were significantly smaller compared to mock-treated of the same genotype.

also had low rates of fetal resorption (3%), indicating that IFN-λ-mediated pregnancy pathology acts through maternal immune cells. Accordingly, we found that decidualized human endometrial cells supported replication of ZIKV and RUBV and responded to IFN-β treatment but did not respond to IFN-λ treatment (see Fig. S4 in the supplemental material). Although IFN-λ signaling induced resorptions, the weights of intact fetuses were no different in poly(I·C)-treated dams than in mock-treated, indicating that poly(I·C) treatment does not induce an IUGR phenotype (Fig. 6F). We also observed IFN-λ-induced resorptions following poly(I·C) administration at E9 and E11 (Fig. 6E), but the effect was

less pronounced than that with treatment at E7, consistent with a model where the pathogenic effects of maternal IFN-λ signaling are most severe earlier in gestation.

DISCUSSION

Our results show that IFN-λ can have both protective and pathogenic effects during pregnancy depending on gestational stage but that both effects occur via signaling in maternal tissues. This identifies a distinct role for IFN-λ compared to IFN-αβ at the maternal-fetal interface, as the pathogenic effects of IFN-αβ act through signaling in fetal tissues in similar ZIKV congenital infection models (29). The contrasting effects of maternal IFN-λ signaling at different gestational stages likely derive from differences in the physiology of the maternal-fetal interface over the course of gestation, producing distinct outcomes when ZIKV infects the maternal-fetal interface prior to placentation (maternal inoculation at E7) or after the placenta has formed (E9 inoculation). We further showed that IFN-λ-mediated pathology is mediated by leukocytes after poly(I·C) treatment. Because the maternal immune landscape varies over gestation, IFN-λ may signal to a leukocyte population that diminishes or changes as pregnancy progresses.

Since IFN-λ is constitutively secreted from human trophoblasts and these cells are refractory to replication by a wide array of viruses and other infectious agents (33–35), we had expected IFN-λ to restrict ZIKV transplacental transmission by signaling on placental trophoblasts and inducing a cell-intrinsic antiviral response. Instead, we found that IFN-λ antiviral activity was mediated through signaling in maternal tissues. Importantly, pregnant and nonpregnant *Ifnlr1*$^{-/-}$ mice showed no differences in viral loads in peripheral tissues (serum, spleen) compared to wild-type mice, consistent with prior studies with other flaviviruses (36, 37) and excluding that enhanced ZIKV transplacental transmission is due to enhanced viral replication and spread in maternal tissues. The mechanism by which maternal IFN-λ signaling restricts ZIKV transplacental transmission remains unclear but could include antiviral activity in the uterine decidua or immunomodulatory effects on maternal leukocytes, such as decidual NK cells, regulatory T cells (Tregs), neutrophils, or dendritic cells. We did not observe IFN-λ responsiveness in a human decidualized endometrial cell line, but decidual cells respond to IFN-λ in other human cell culture models, including explants and organoids (8, 9). Differences in decidual responsiveness have been noted from cell models taken at different times in gestation (38) and could explain the lack of IFN-λ responsiveness that we observed in a decidual cell line. Although we did not find a role for fetal IFN-λ signaling, human placental models do respond to IFN-λ in culture. Differences in placental IFN-λ responsiveness could be due to variations in the mouse and human placentas. Although both are discoid and hemochorial, mouse and human placentas have distinct trophoblast lineages, which include trophoblast giant cells and a second layer of syncytiotrophoblasts in mice and extravillous trophoblasts in humans (30).

In contrast to the protective effect of IFN-λ that we observed after E9 infection, IFN-λ signaling enhanced transplacental transmission in mice infected at E7. Consistent with a pathogenic effect of IFN-λ earlier in gestation, IFN-λ signaling increased fetal resorption rates after E7 infections in mice that sustain high ZIKV replication (*Ifnar1*$^{-/-}$), although there were no significant differences in rates of transplacental transmission or viral loads in the fetuses that were not resorbed. Interestingly, IFN-λ activity induced resorption of approximately one in three fetuses, and we observed a similar effect on transplacental transmission, with an additional one-third of fetuses exhibiting transmission in the context of maternal IFN-λ signaling (transmission to 47% of fetuses from *Ifnlr1*$^{+/-}$ dams compared to 13% from *Ifnlr1*$^{-/-}$ dams). Remarkably, the pathogenic effects of IFN-λ were mediated exclusively by signaling in maternal tissues, similar to the protective effects of IFN-λ. The pathogenic effects of IFN-λ did not require ZIKV infection, as we could elicit a similar phenotype by treating pregnant dams with poly(I·C).

We found that rates of IFN-λ-mediated pathology were greatest when poly(I·C) was administered earlier in gestation, and we predict that enhanced ZIKV transmission and fetal pathology after E7 infection results from pathogenic effects of IFN-λ signaling on the placental barrier, which is not yet fully formed at this stage of gestation. We did not determine the gestation range over which the effects of IFN-λ are pathogenic rather than protective, but doing so will be valuable in defining the cellular targets and mechanism by which IFN-λ is acting at the maternal-fetal interface. Congenital viral infections also produce fetal pathology with gestational stage-dependent effects in humans: congenital rubella syndrome almost entirely results from infection in the first trimester, and ZIKV and (HCMV) infections early in pregnancy likewise produce the most severe outcomes, although ZIKV and HCMV can be pathogenic throughout pregnancy (1). Our findings emphasize the importance of studying congenital infections and immune responses at different gestational stages. One limitation of this study is that it does not include infections at time points following placentation, so it remains to be determined how IFN-λ affects pregnancies late in gestation. Furthermore, congenital infections can result from both transplacental spread and ascending infection from the vagina. The immunologic and anatomical barriers to ascending infection are different from those to transplacental infection, so IFN-λ could have distinct effect based on the route of infection.

We found that fetuses were protected from resorption when IFN-λ signaling was ablated only in hematopoietic cells, indicating that IFN-λ pathogenic effects result from signaling in maternal leukocytes. Since IFN-λ-mediated pathology depends on gestational stage, IFN-λ may act through particular leukocytes present earlier in gestation that diminish over time. Early in gestation, 40% of the maternal decidua is made up of leukocytes including NK cells, macrophages, and Tregs (2). These populations change over the course of gestation and play a critical role in mediating placental invasion and spiral artery formation. IFN-λ signals to several of these cell types in contexts outside of pregnancy (39) and potentially could disturb the immune balance necessary for proper placentation. Multiple distinct subsets of macrophages have been identified in the maternal decidua, and imbalance between macrophages subtypes is associated with adverse pregnancy outcomes (40, 41). IFN-λ changes the transcriptional profile and increases proinflammatory phenotypes of monocytes differentiated into macrophages in culture (42, 43). Macrophages skew toward an M2 phenotype as pregnancy progresses, and IFN-λ could increase proportions of M1 macrophages, potentially leading to inflammation and fetal rejection. Placentas harvested from ZIKV-infected rhesus macaques have more monocytes and macrophages than those from uninfected animals, as well as changes in the proportions of monocyte subsets (44). Although a function for neutrophils at the maternal-fetal interface has not been well defined, mouse neutrophils do respond to IFN-λ. However, IFN-λ has anti-inflammatory activity in these contexts and is associated with reductions in inflammatory pathology during influenza infection as well as rheumatoid arthritis (45, 46). Further research focusing on identifying the specific maternal cell types that respond to IFN-λ signaling will enhance our understanding of the mechanisms underlying IFN-λ-mediated fetal pathology.

We found a striking sex difference in IFN-λ-mediated pathology, with male fetuses exhibiting significantly higher resorption rates than female fetuses. This observation is consistent with immune-mediated rejection, as only male fetuses are genetically distinct from the dam in these congenic pregnancies. Immunity at the maternal-fetal interface is carefully regulated to prevent non-self-rejection of the fetus and includes mechanisms that downregulate NK cell cytotoxicity and recognition of non-self-tissues (2). Modeling congenital infection in semi-allogeneic pregnancies will provide further insight into the role of IFN-λ signaling in changes to maternal immune tolerance.

Although IFN-λ is best characterized for its protective activity in the context of viral infections, particularly in the respiratory and gastrointestinal tracts (5), IFN-λ signaling

also is associated with deleterious effects in some other contexts. IFN-λ contributes to impaired tissue repair following respiratory and gastrointestinal infections in mice (47–49). In humans, multiple polymorphisms in the IFN-λ locus are associated with clinical outcomes from hepatitis C virus (HCV) infection (50). Among these, a frameshift mutation in the promoter of *IFNL4* results in the loss of IFN-λ4 production and concomitant improved clearance of HCV as well as other gastrointestinal and respiratory infections though the mechanism by which the loss of an IFN results in an improved antiviral response remains unclear (51, 52). The pseudogenization of IFN-λ4, along with selection for lower-potency variants, suggest IFN-λ4 signaling has been deleterious during human evolution (53, 54). In mice, the IFN-λ family consists only of IFN-λ2 and IFN-λ3, as IFN-λ1 is a pseudogene and the genomic region encoding IFN-λ4 is absent (55, 56), which limits some comparisons of the effects of IFN-λ in mice and humans.

Our observations of a pathogenic effect of IFN-λ signaling at the maternal-fetal interface bear some similarity to the pathogenic effects of IFN-αβ in pregnancy, though notably in mouse models of congenital ZIKV infection, IFN-αβ is pathogenic when it signals to fetal tissues (29), whereas we find that IFN-λ acts through signaling in maternal tissues. Women with dysregulated IFN-αβ signaling (sustained IFN production or impaired receptor downregulation) exhibit poor pregnancy outcomes, including preeclampsia as well as neurodevelopmental defects similar to those induced by congenital infection, consistent with a role for dysregulated IFN-αβ responses in placental damage (57–61). Whether dysregulated IFN-λ signaling exerts similar effects during human pregnancy remains to be determined.

Altogether, these findings identify an unexpected effect of IFN-λ signaling specifically in maternal (rather than placental or fetal) tissues, which is distinct from the pathogenic effects of IFN-αβ during pregnancy. These results highlight the complexity of immune signaling at the maternal-fetal interface, where disparate outcomes can result from signaling at different gestational stages.

MATERIALS AND METHODS

Viruses. Virus stocks were grown in Vero cells in Dulbecco's modified Eagle medium (DMEM) containing 5% fetal bovine serum (FBS), L-glutamine, and HEPES at 37°C with 5% CO_2. ZIKV strain FSS13025 (Cambodia 2010) was obtained from the World Reference Center for Emerging Viruses and Arboviruses (62). ZIKV strains PRVABC59 (Puerto Rico 2015) and H/PF/2013 (French Polynesia 2013) were obtained from the U.S. CDC (63, 64). RUBV strain M33 was obtained from Dr. Michael Rossmann (Purdue University) (65). DENV4 (TVP-360) was obtained from Dr. Aravinda DeSilva (UNC Chapel Hill). Virus stock titer was quantified by focus-forming assay on Vero cells (66). Viral foci were detected using 500 ng/mL of anti-flavivirus mouse monoclonal antibody E60 (67) or 1:1,000 dilution of goat anti-RUBV antibody (Lifespan Biosciences; LC-C103273), 1:5,000 dilution of a horseradish peroxidase (HRP)-conjugated goat anti-mouse IgG (Sigma; no. A8924), or 1:5,000 dilution of an HRP-conjugated rabbit anti-goat (Sigma; no. A5420), and TrueBlue peroxidase substrate (KPL). Antibody incubations were performed overnight at 4°C. Foci were counted on a CTL ImmunoSpot analyzer.

Mice. All experiments and husbandry were performed under the approval of the University of North Carolina at Chapel Hill Institutional Animal Care and Use Committee. Experiments used 8- to 20-week-old female mice on a C57BL/6 background. Wild-type mice were obtained commercially (Jackson Labs; 000664) or bred in-house. *Ifnar1*$^{-/-}$ and *Ifnar1*$^{-/-}$ *Ifngr1*$^{-/-}$ mice were obtained from Dr. Jason Whitmire (UNC Chapel Hill) then bred in-house. *Ifnlr1*$^{-/-}$ mice were provided by Dr. Herbert Virgin (Washington University in St. Louis), generated by crossing *Ifnlr1*$^{fl/fl}$ mice with mice constitutively expressing Cre recombinase under a CMV promoter (68); these mice were then bred in-house as knockout × knockout (37). *Ifnar1*$^{-/-}$ *Ifnlr1*$^{-/-}$ DKO mice were generated by crossing *Ifnlr1*$^{-/-}$ and *Ifnar1*$^{-/-}$ mice. *Ifnlr1*$^{+/-}$ mice were generated by crossing *Ifnlr1*$^{-/-}$ and wild-type mice. *Vav*-Cre *Ifnlr1*$^{-/-}$ mice were generated by crossing *Ifnlr1*$^{fl/fl}$ mice with mice expressing Cre recombinase under the *Vav* promoter (Jackson labs; 008610) and bred as Cre hemizygotes with Cre maintained on the female breeder.

Mouse experiments. Timed pregnancies were set up by exposing females to soiled male cage bedding for 3 days to promote estrus, then housing single pairs of male and female mice overnight (E0), and separating males and females the next morning (E1). Mice were infected by a subcutaneous route in the footpad with 1,000 FFU of ZIKV in 50 μL. Wild-type, *Ifnlr1*$^{+/-}$, and *Ifnlr1*$^{-/-}$ mice were administered 2 mg of anti-IFNAR1-blocking antibody MAR1-5A3 by intraperitoneal injection (26). For viral load experiments in nonpregnant mice, blood was collected at 2 or 4 days postinfection (dpi) by submandibular bleed or at 6 dpi by cardiac puncture into serum separator tubes (BD), and serum was separated by centrifugation in a microfuge at 8,000 rpm for 5 min. Spleen, brain, and uterus were collected 6 dpi following perfusion with 20 mL of phosphate-buffered saline (PBS). For weight loss and survival experiments, mice were weighed each day following infection. Pregnant mice were sacrificed at E15 (6 or 8 dpi).

Maternal blood was collected by cardiac puncture in serum separator tubes (BD), and serum was separated by centrifugation in a microfuge at 8,000 rpm for 5 min. Dams were perfused with 20 mL of PBS and then fetal heads, fetal bodies, and their associated placentas, as well as maternal spleen and brain were collected. Fetal tissues were weighed, and total fetal weight was determined by combining fetal head and body weights. Photographs of fetuses and uteruses were taken at time of harvest, and crown rump length was measured using ImageJ (69). For poly(I·C) experiments, 200 μg of low-molecular-weight poly(I·C) (InvivoGen; tlrl-picw) was administered by intraperitoneal injection at the indicated days following mating. At E15, pregnant dams were sacrificed and whole fetuses and their associated placentas were collected and weighed. Implantations with no discernible placentas or fetuses were classified as resorptions.

RUBV mouse experiments. *Ifnar1*$^{-/-}$, *Ifnlr1*$^{-/-}$, *Ifnar1*$^{-/-}$ *Ifngr1*$^{-/-}$ DKO, and wild-type mice were inoculated with 1,000 or 1 × 10^5 FFU of RUBV by subcutaneous injection in the footpad or intranasal administration. Weights were monitored for 14 dpi. For viral load experiments, serum and whole blood were harvested 2, 4, and 7 dpi by submandibular bleed into serum separator tubes (BD), and serum was separated by centrifugation in a microfuge at 8,000 rpm for 5 min. Mice were sacrificed at 7 dpi, perfused with 20 mL of PBS, then spleens, lung, and brains were harvested.

Viral loads. Tissues were homogenized in 600 μL of PBS using a MagNA Lyser (Roche), and then 150 μL of homogenate was added to an equal volume of buffer RLT (Qiagen) for RNA extraction. Viral RNA was extracted using a Qiagen RNeasy kit (tissues) or Qiagen viral RNA minikit (serum). ZIKV RNA was detected by TaqMan one-step qRT-PCR using the following primer probe set: forward-CCGCTGCCCAACACAAG; reverse-CCACTAACGTTCTTTTGCAGACAT; probe56-FAM/AGCCTACCT/ZEN/TGACAAGCAATCAGACACTCAA/3IABkFQ on a Bio-Rad CFX96 using standard cycling conditions. ZIKV genome equivalents per milliliter were determined compared to a ZIKV standard curve of 100-fold dilutions of ZIKV-A plasmid (70) or 100-fold dilutions of RNA extracted from viral stock. RUBV viral loads were determined compared to a standard curve made from 100-fold dilutions of RNA isolated from virus stock.

IFN-λ activity assay. Tissue homogenates and serum were diluted 1:4 in PBS, and 20 μL was added to 96-well plates. HEK-Blue IFN-λ reporter cells (InvivoGen) were then suspended at a concentration of 2.8 × 10^5 cells/mL in DMEM supplemented with 1 μg/mL puromycin, 10 μg/mL blasticidin, and 100 μg/mL zeocin. The HEK-Blue IFN-λ cell suspension was then added to each well of diluted tissue samples and incubated at 37°C for 24 h. Then, 20 μL of the culture medium was added to QUANTI-Blue substrate (InvivoGen) for 1.5 h, and absorbance was measured at 620 nm (BioTek; Epoch). Absorbance readings were converted to concentration using a standard curve of 10-fold serial dilutions of hIFN-λ2 (PBL11820-1) starting at 2,500 ng/mL, which was run concurrently with tissue samples.

IFN-β ELISA. Tissues were homogenized in 600 μL of PBS using a MagNA Lyser (Roche). Tissue and serum samples were loaded directly onto enzyme-linked immunosorbent assay (ELISA) plates according to protocol (BioLegend; 439407 Legend Max Mouse IFN-β ELISA kit). Absorbance was read at 450 nm (BioTek; Epoch).

Genotyping. *Ifnlr1* and *Sry* (fetal sex) genotypes were determined by PCR on fetal head RNA samples (which contain copurified genomic DNA) or on DNA extracted from maternal blood and tail samples using the Quantabio supermix and the following previously described primers: *Ifnlr1* $F_1$5-AGGGAAGCCAAGGGGATGGC-3′, $R_1$5-AGTGCCTGCTGAGGACCAGGA-3′, $R_2$5-GGCTCTGGACCTACGCGCTG-3′ (68), *Sry* F5-TTGTCTAGAGAGCATGGAGGGCCAT-3′, and R5-CCACTCCTCTGTGAC ACTTTAGCCCT-3′ (71).

Viral replication and IFN response assays. Human endometrial stromal cells (HESC-T) were obtained from David Aronoff (Vanderbilt University). HESC-T were decidualized by culturing cells with 0.5 mM 8-bromo-cAMP (Sigma B5386), 1 μM medroxyprogesterone acetate (MPA) (Sigma; M1629), 10 nM 17b-estradiol-acetate (estrogen E2, Sigma E7879) for 5 days as originally described (72). Cells were plated at 500,000 cells/well in 6-well plates and infected at a multiplicity of infection (MOI) of 1 with ZIKV (H/PF/2013), DENV4 (TVP-360), or RUBV (M33) in 300 μL/well. Supernatant was collected at 4, 24, 48, and 72 h postinfection and titered by focus forming assay as described above. A549, JEG3, HTR8, and decidualized T-HESC were treated with 50 ng/mL IFN-λ (PBL11820-1) or 5 ng/mL IFN-β (PBL11420-1) or infected with ZIKV (H/PF/2013) or DENV4 (TVP-360) at an MOI of 1. After 24 h, RNA was extracted from cell lysates (Qiagen RNeasy kit), and *IFIT1* expression was measured by qRT-PCR (IDT; assay ID Hs.PT.561.20769090.g).

Statistics. All statistics were performed using GraphPad Prism. Significant differences in fetal weights, viral loads with standard distributions (maternal spleens, placentas), and placental IFN-λ levels were assessed by analysis of variance (ANOVA) or *t* test. Significant differences in fetal-head viral loads were calculated by Mann-Whitney. In experiments where we performed multiple comparisons, groups that are significantly different from one another are denoted by different italicized letters.

SUPPLEMENTAL MATERIAL

Supplemental material is available online only.

FIG S1, TIF file, 0.1 MB.

FIG S2, TIF file, 0.2 MB.

FIG S3, TIF file, 0.3 MB.

FIG S4, TIF file, 0.1 MB.

ACKNOWLEDGMENTS

This work was supported by R01 AI139512 and R21 AI129431 (H.M.L.) and start-up funds from UNC Chapel Hill Department of Microbiology and Immunology and the Lineberger Comprehensive Cancer Center. R.L.C. and D.T.P. were supported by T32 AI007419; R.L.C. was supported by a UNC dissertation completion fellowship.

REFERENCES

1. Megli CJ, Coyne CB. 2022. Infections at the maternal–fetal interface: an overview of pathogenesis and defence. Nat Rev Microbiol 20:67–82. https://doi.org/10.1038/s41579-021-00610-y.
2. Mor G, Aldo P, Alvero AB. 2017. The unique immunological and microbial aspects of pregnancy. Nat Rev Immunol 17:469–482. https://doi.org/10.1038/nri.2017.64.
3. Murphy SP, Tayade C, Ashkar AA, Hatta K, Zhang J, Croy BA. 2009. Interferon gamma in successful pregnancies. Biol Reprod 80:848–859. https://doi.org/10.1095/biolreprod.108.073353.
4. Zhou JZ, Way SS, Chen K. 2018. Immunology of the uterine and vaginal mucosae. Trends Immunol 39:302–314. https://doi.org/10.1016/j.it.2018.01.007.
5. Lazear HM, Schoggins JW, Diamond MS. 2019. Shared and distinct functions of type I and type III interferons. Immunity 50:907–923. https://doi.org/10.1016/j.immuni.2019.03.025.
6. Bayer A, Lennemann NJ, Ouyang Y, Bramley JC, Morosky S, Marques ETDA, Cherry S, Sadovsky Y, Coyne CB. 2016. Type III interferons produced by human placental trophoblasts confer protection against Zika virus infection. Cell Host Microbe 19:705–712. https://doi.org/10.1016/j.chom.2016.03.008.
7. Corry J, Arora N, Good CA, Sadovsky Y, Coyne CB. 2017. Organotypic models of type III interferon-mediated protection from Zika virus infections at the maternal–fetal interface. Proc Natl Acad Sci U S A 114:9433–9438. https://doi.org/10.1073/pnas.1707513114.
8. Yang L, Megli C, Coyne CB. 2021. Innate immune signaling in trophoblast and decidua organoids defines differential antiviral defenses at the maternal-fetal interface. bioRxiv https://doi.org/10.1101/2021.03.29.437467.
9. Jagger BW, Miner JJ, Cao B, Arora N, Smith AM, Kovacs A, Mysorekar IU, Coyne CB, Diamond MS. 2017. Gestational stage and IFN-λ signaling regulate ZIKV infection in utero. Cell Host Microbe 22:366–376. https://doi.org/10.1016/j.chom.2017.08.012.
10. Pierson TC, Diamond MS. 2018. The emergence of Zika virus and its new clinical syndromes. Nature 560:573–581. https://doi.org/10.1038/s41586-018-0446-y.
11. Platt DJ, Miner JJ. 2017. Consequences of congenital Zika virus infection. Curr Opin Virol 27:1–7. https://doi.org/10.1016/j.coviro.2017.09.005.
12. Mulkey SB, Arroyave-Wessel M, Peyton C, Bulas DI, Fourzali Y, Jiang J, Russo S, McCarter R, Msall ME, Du Plessis AJ, Debiasi RL, Cure C. 2020. Neurodevelopmental abnormalities in children with in utero Zika virus exposure without congenital Zika syndrome. JAMA Pediatr 174:269–276. https://doi.org/10.1001/jamapediatrics.2019.5204.
13. Valdes V, Zorrilla CD, Gabard-Durnam L, Muler-Mendez N, Rahman ZI, Rivera D, Nelson CA. 2019. Cognitive development of infants exposed to the Zika virus in Puerto Rico. JAMA Netw Open 2:e1914061. https://doi.org/10.1001/jamanetworkopen.2019.14061.
14. Stringer EM, Martinez E, Blette B, Toval Ruiz CE, Boivin M, Zepeda O, Stringer JSA, Morales M, Ortiz-Pujols S, Familiar I, Collins M, Chavarria M, Goldman B, Bowman N, De Silva A, Westreich D, Hudgens M, Becker-Dreps S, Bucardo F. 2021. Neurodevelopmental outcomes of children following in utero exposure to Zika in Nicaragua. Clin Infect Dis 72:E146–E153. https://doi.org/10.1093/cid/ciaa1833.
15. Yockey LJ, Varela L, Rakib T, Khoury-Hanold W, Fink SL, Stutz B, Szigeti-Buck K, Van den Pol A, Lindenbach BD, Horvath TL, Iwasaki A. 2016. Vaginal exposure to Zika virus during pregnancy leads to fetal brain infection. Cell 166:1247–1256. https://doi.org/10.1016/j.cell.2016.08.004.
16. Miner JJ, Cao B, Govero J, Smith AM, Fernandez E, Cabrera OH, Garber C, Noll M, Klein RS, Noguchi KK, Mysorekar IU, Diamond MS. 2016. Zika virus infection during pregnancy in mice causes placental damage and fetal demise. Cell 165:1081–1091. https://doi.org/10.1016/j.cell.2016.05.008.
17. Narasimhan H, Chudnovets A, Burd I, Pekosz A, Klein SL. 2020. Animal models of congenital Zika syndrome provide mechanistic insight into viral pathogenesis during pregnancy. PLoS Negl Trop Dis 14:e0008707. https://doi.org/10.1371/journal.pntd.0008707.
18. Vermillion MS, Lei J, Shabi Y, Baxter VK, Crilly NP, McLane M, Griffin DE, Pekosz A, Klein SL, Burd I. 2017. Intrauterine Zika virus infection of pregnant immunocompetent mice models transplacental transmission and adverse perinatal outcomes. Nat Commun 8:14575. https://doi.org/10.1038/ncomms14575.
19. Honein MA, Dawson AL, Petersen EE, Jones AM, Lee EH, Yazdy MM, Ahmad N, Macdonald J, Evert N, Bingham A, Ellington SR, Shapiro-Mendoza CK, Oduyebo T, Fine AD, Brown CM, Sommer JN, Gupta J, Cavicchia P, Slavinski S, White JL, Owen SM, Petersen LR, Boyle C, Meaney-Delman D, Jamieson DJ, US Zika Pregnancy Registry Collaboration. 2017. Birth defects among fetuses and infants of US women with evidence of possible Zika virus infection during pregnancy. JAMA 317:59–68. https://doi.org/10.1001/jama.2016.19006.
20. Brady OJ, Osgood-Zimmerman A, Kassebaum NJ, Ray SE, De Araùjo VEM, Da Nóbrega AA, Frutuoso LCV, Lecca RCR, Stevens A, De Oliveira BZ, De Lima JM, Bogoch II, Mayaud P, Jaenisch T, Mokdad AH, Murray CJL, Hay SI, Reiner RC, Marinho F. 2019. The association between Zika virus infection and microcephaly in Brazil 2015–2017: an observational analysis of over 4 million births. PLoS Med 16:e1002755. https://doi.org/10.1371/journal.pmed.1002755.
21. Hoen B, Schaub B, Funk AL, Ardillon V, Boullard M, Cabié A, Callier C, Carles G, Cassadou S, Césaire R, Douine M, Herrmann-Storck C, Kadhel P, Laouénan C, Madec Y, Monthieux A, Nacher M, Najioullah F, Rousset D, Ryan C, Schepers K, Stegmann-Planchard S, Tressières B, Voluménie J-L, Yassinguezo S, Janky E, Fontanet A. 2018. Pregnancy outcomes after ZIKV infection in French territories in the Americas. N Engl J Med 378:985–994. https://doi.org/10.1056/NEJMoa1709481.
22. Ospina ML, Tong VT, Gonzalez M, Valencia D, Mercado M, Gilboa SM, Rodriguez AJ, Tinker SC, Rico A, Winfield CM, Pardo L, Thomas JD, Avila G, Villanueva JM, Gomez S, Jamieson DJ, Prieto F, Meaney-Delman D, Pacheco O, Honein MA. 2020. Zika virus disease and pregnancy outcomes in Colombia. N Engl J Med 383:537–545. https://doi.org/10.1056/NEJMoa1911023.
23. Ander SE, Diamond MS, Coyne CB. 2019. Immune responses at the maternal-fetal interface. Sci Immunol 4:eaat6114. https://doi.org/10.1126/sciimmunol.aat6114.
24. Grant A, Ponia SS, Tripathi S, Balasubramaniam V, Miorin L, Sourisseau M, Schwarz MC, Sánchez-Seco MP, Evans MJ, Best SM, García-Sastre A. 2016. Zika virus targets human STAT2 to inhibit type I interferon signaling. Cell Host Microbe 19:882–890. https://doi.org/10.1016/j.chom.2016.05.009.
25. Tripathi S, Balasubramaniam VRMT, Brown JA, Mena I, Grant A, Bardina SV, Maringer K, Schwarz MC, Maestre AM, Sourisseau M, Albrecht RA, Krammer F, Evans MJ, Fernandez-Sesma A, Lim JK, García-Sastre A. 2017. A novel Zika virus mouse model reveals strain specific differences in virus pathogenesis and host inflammatory immune responses. PLoS Pathog 13:e1006258. https://doi.org/10.1371/journal.ppat.1006258.
26. Lazear HM, Govero J, Smith AM, Platt DJ, Fernandez E, Miner JJ, Diamond MS. 2016. A mouse model of Zika virus pathogenesis. Cell Host Microbe 19:720–730. https://doi.org/10.1016/j.chom.2016.03.010.
27. Caine E, Jagger B, Diamond M. 2018. Animal models of Zika virus infection during pregnancy. Viruses 10:598. https://doi.org/10.3390/v10110598.
28. Carbaugh DL, Zhou S, Sanders W, Moorman NJ, Swanstrom R, Lazear HM. 2020. Two genetic differences between closely related Zika virus strains determine pathogenic outcome in mice. J Virol 94:e00618-20. https://doi.org/10.1128/JVI.00618-20.
29. Yockey LJ, Jurado KA, Arora N, Millet A, Rakib T, Milano KM, Hastings AK, Fikrig E, Kong Y, Horvath TL, Weatherbee S, Kliman HK, Coyne CB, Iwasaki A. 2018. Type I interferons instigate fetal demise after Zika virus infection. Sci Immunol 3:eaao1680. https://doi.org/10.1126/sciimmunol.aao1680.
30. Hemberger M, Hanna CW, Dean W. 2020. Mechanisms of early placental development in mouse and humans. Nat Rev Genet 21:27–43. https://doi.org/10.1038/s41576-019-0169-4.
31. Croy BA, Yamada AT, DeMayo FJ, Adamson SL (ed). 2014. The guide to investigation of mouse pregnancy. Academic Press, San Diego, CA.

32. Banatvala JE, Brown DWG. 2004. Rubella. Lancet 363:1127–1137. https://doi.org/10.1016/S0140-6736(04)15897-2.
33. Delorme-Axford E, Donker RB, Mouillet J-F, Chu T, Bayer A, Ouyang Y, Wang T, Stolz DB, Sarkar SN, Morelli AE, Sadovsky Y, Coyne CB. 2013. Human placental trophoblasts confer viral resistance to recipient cells. Proc Natl Acad Sci U S A 110:12048–12053. https://doi.org/10.1073/pnas.1304718110.
34. Bayer A, Delorme-Axford E, Sleigher C, Frey TK, Trobaugh DW, Klimstra WB, Emert-Sedlak LA, Smithgall TE, Kinchington PR, Vadia S, Seveau S, Boyle JP, Coyne CB, Sadovsky Y. 2015. Human trophoblasts confer resistance to viruses implicated in perinatal infection. Am J Obstet Gynecol 212:71.e1–71.e8. https://doi.org/10.1016/j.ajog.2014.07.060.
35. Ander SE, Rudzki EN, Arora N, Sadovsky Y, Coyne CB, Boyle JP. 2018. Human placental syncytiotrophoblasts restrict Toxoplasma gondii attachment and replication and respond to infection by producing immunomodulatory chemokines. mBio 9:e01678-17. https://doi.org/10.1128/mBio.01678-17.
36. Douam F, Soto Albrecht YE, Hrebikova G, Sadimin E, Davidson C, Kotenko SV, Ploss A. 2017. Type III interferon-mediated signaling is critical for controlling live attenuated yellow fever virus infection *in vivo*. mBio 8:e00819-17. https://doi.org/10.1128/mBio.00819-17.
37. Lazear HM, Daniels BP, Pinto AK, Huang AC, Vick SC, Doyle SE, Gale M, Klein RS, Diamond MS. 2015. Interferon-λ restricts West Nile virus neuroinvasion by tightening the blood-brain barrier. Sci Transl Med 7:284ra57. https://doi.org/10.1126/scitranslmed.aaa4304.
38. Guzeloglu-Kayisli O, Guo X, Tang Z, Semerci N, Ozmen A, Larsen K, Mutluay D, Guller S, Schatz F, Kayisli UA, Lockwood CJ. 2020. Zika virus–infected decidual cells elicit a gestational age–dependent innate immune response and exaggerate trophoblast Zika permissiveness: implication for vertical transmission. J Immunol 205:3083–3094. https://doi.org/10.4049/jimmunol.2000713.
39. Zanoni I, Granucci F, Broggi A. 2017. Interferon (IFN)-λ takes the helm: immunomodulatory roles of type III IFNs. Front Immunol 8:1661. https://doi.org/10.3389/fimmu.2017.01661.
40. Jiang X, Du M-R, Li M, Wang H. 2018. Three macrophage subsets are identified in the uterus during early human pregnancy. Cell Mol Immunol 15:1027–1037. https://doi.org/10.1038/s41423-018-0008-0.
41. Ning F, Liu H, Lash GE. 2016. The role of decidual macrophages during normal and pathological pregnancy. Am J Reprod Immunol 75:298–309. https://doi.org/10.1111/aji.12477.
42. De M, Bhushan A, Chinnaswamy S. 2021. Monocytes differentiated into macrophages and dendritic cells in the presence of human IFN-λ3 or IFN-λ4 show distinct phenotypes. J Leukoc Biol 110:357–374. https://doi.org/10.1002/JLB.3A0120-001RRR.
43. Read SA, Wijaya R, Ramezani-Moghadam M, Tay E, Schibeci S, Liddle C, Lam VWT, Yuen L, Douglas MW, Booth D, George J, Ahlenstiel G. 2019. Macrophage coordination of the interferon lambda immune response. Front Immunol 10:2674. https://doi.org/10.3389/fimmu.2019.02674.
44. Hirsch AJ, Roberts VHJ, Grigsby PL, Haese N, Schabel MC, Wang X, Lo JO, Liu Z, Kroenke CD, Smith JL, Kelleher M, Broeckel R, Kreklywich CN, Parkins CJ, Denton M, Smith P, DeFilippis V, Messer W, Nelson JA, Hennebold JD, Grafe M, Colgin L, Lewis A, Ducore R, Swanson T, Legasse AW, Axthelm MK, MacAllister R, Moses AV, Morgan TK, Frias AE, Streblow DN. 2018. Zika virus infection in pregnant rhesus macaques causes placental dysfunction and immunopathology. Nat Commun 9:263. https://doi.org/10.1038/s41467-017-02499-9.
45. Galani IE, Triantafyllia V, Eleminiadou E-E, Koltsida O, Stavropoulos A, Manioudaki M, Thanos D, Doyle SE, Kotenko SV, Thanopoulou K, Andreakos E. 2017. Interferon-λ mediates non-redundant front-line antiviral protection against influenza virus infection without compromising host fitness. Immunity 46:875–890. https://doi.org/10.1016/j.immuni.2017.04.025.
46. Goel RR, Kotenko SV, Kaplan MJ. 2021. Interferon lambda in inflammation and autoimmune rheumatic diseases. Nat Rev Rheumatol 17:349–362. https://doi.org/10.1038/s41584-021-00606-1.
47. Major J, Crotta S, Llorian M, McCabe TM, Gad HH, Priestnall SL, Hartmann R, Wack A. 2020. Type I and III interferons disrupt lung epithelial repair during recovery from viral infection. Science 369:712–717. https://doi.org/10.1126/science.abc2061.
48. Broggi A, Ghosh S, Sposito B, Spreafico R, Balzarini F, Lo Cascio A, Clementi N, de Santis M, Mancini N, Granucci F, Zanoni I. 2020. Type III interferons disrupt the lung epithelial barrier upon viral recognition. Science 369:706–712. https://doi.org/10.1126/science.abc3545.
49. McElrath C, Espinosa V, Lin J-D, Peng J, Sridhar R, Dutta O, Tseng H-C, Smirnov SV, Risman H, Sandoval MJ, Davra V, Chang Y-J, Pollack BP, Birge RB, Galan M, Rivera A, Durbin JE, Kotenko SV. 2021. Critical role of interferons in gastrointestinal injury repair. Nat Commun 12:2624. https://doi.org/10.1038/s41467-021-22928-0.
50. Griffiths SJ, Dunnigan CM, Russell CD, Haas JG. 2015. The role of interferon-λ locus polymorphisms in hepatitis C and other infectious diseases. J Innate Immun 7:231–242. https://doi.org/10.1159/000369902.
51. Prokunina-Olsson L, Morrison RD, Obajemu A, Mahamar A, Kim S, Attaher O, Florez-Vargas O, Sidibe Y, Onabajo OO, Hutchinson AA, Manning M, Kwan J, Brand N, Dicko A, Fried M, Albert PS, Mbulaiteye SM, Duffy PE. 2021. IFN-λ4 is associated with increased risk and earlier occurrence of several common infections in African children. Genes Immun 22:44–55. https://doi.org/10.1038/s41435-021-00127-7.
52. Prokunina-Olsson L, Muchmore B, Tang W, Pfeiffer RM, Park H, Dickensheets H, Hergott D, Porter-Gill P, Mumy A, Kohaar I, Chen S, Brand N, Tarway M, Liu L, Sheikh F, Astemborski J, Bonkovsky HL, Edlin BR, Howell CD, Morgan TR, Thomas DL, Rehermann B, Donnelly RP, O'Brien TR. 2013. A variant upstream of IFNL3 (IL28B) creating a new interferon gene IFNL4 is associated with impaired clearance of hepatitis C virus. Nat Genet 45:164–171. https://doi.org/10.1038/ng.2521.
53. Key FM, Peter B, Dennis MY, Huerta-Sánchez E, Tang W, Prokunina-Olsson L, Nielsen R, Andrés AM. 2014. Selection on a variant associated with improved viral clearance drives local, adaptive pseudogenization of interferon lambda 4 (IFNL4). PLoS Genet 10:e1004681. https://doi.org/10.1371/journal.pgen.1004681.
54. Bamford CGG, Aranday-Cortes E, Filipe IC, Sukumar S, Mair D, Filipe ADS, Mendoza JL, Garcia KC, Fan S, Tishkoff SA, McLauchlan J. 2018. A polymorphic residue that attenuates the antiviral potential of interferon lambda 4 in hominid lineages. PLoS Pathog 14:e1007307. https://doi.org/10.1371/journal.ppat.1007307.
55. Kotenko SV, Durbin JE. 2017. Contribution of type III interferons to antiviral immunity: location, location, location. J Biol Chem 292:7295–7303. https://doi.org/10.1074/jbc.R117.777102.
56. Wack A, Terczyńska-Dyla E, Hartmann R. 2015. Guarding the frontiers: the biology of type III interferons. Nat Immunol 16:802–809. https://doi.org/10.1038/ni.3212.
57. Andrade D, Kim M, Blanco LP, Karumanchi SA, Koo GC, Redecha P, Kirou K, Alvarez AM, Mulla MJ, Crow MK, Abrahams VM, Kaplan MJ, Salmon JE. 2015. Interferon-α and angiogenic dysregulation in pregnant lupus patients who develop preeclampsia. Arthritis Rheumatol 67:977–987. https://doi.org/10.1002/art.39029.
58. Crow YJ, Manel N. 2015. Aicardi–Goutières syndrome and the type I interferonopathies. Nat Rev Immunol 15:429–440. https://doi.org/10.1038/nri3850.
59. Meuwissen MEC, Schot R, Buta S, Oudesluijs G, Tinschert S, Speer SD, Li Z, van Unen L, Heijsman D, Goldmann T, Lequin MH, Kros JM, Stam W, Hermann M, Willemsen R, Brouwer RWW, Van IJcken WFJ, Martin-Fernandez M, de Coo I, Dudink J, de Vries FAT, Bertoli Avella A, Prinz M, Crow YJ, Verheijen FW, Pellegrini S, Bogunovic D, Mancini GMS. 2016. Human USP18 deficiency underlies type 1 interferonopathy leading to severe pseudo-TORCH syndrome. J Exp Med 213:1163–1174. https://doi.org/10.1084/jem.20151529.
60. Sanchis A, Cerveró L, Bataller A, Tortajada JL, Huguet J, Crow YJ, Ali M, Higuet LJ, Martínez-Frías ML. 2005. Genetic syndromes mimic congenital infections. J Pediatr 146:701–705. https://doi.org/10.1016/j.jpeds.2005.01.033.
61. Casazza RL, Lazear HM, Miner JJ. 2020. Protective and pathogenic effects of interferon signaling during pregnancy. Viral Immunol 33:3–11. https://doi.org/10.1089/vim.2019.0076.
62. Heang V, Yasuda CY, Sovann L, Haddow AD, da Rosa APT, Tesh RB, Kasper MR. 2012. Zika virus infection, Cambodia, 2010. Emerg Infect Dis 18:349–351. https://doi.org/10.3201/eid1802.111224.
63. Lanciotti RS, Lambert AJ, Holodniy M, Saavedra S, del Carmen Castillo Signor L. 2016. Phylogeny of Zika virus in western hemisphere, 2015. Emerg Infect Dis 22:933–935. https://doi.org/10.3201/eid2205.160065.
64. Baronti C, Piorkowski G, Charrel RN, Boubis L, Leparc-Goffart I, de Lamballerie X. 2014. Complete coding sequence of Zika virus from a French Polynesia outbreak in 2013. Genome Announc 2:e00500-14. https://doi.org/10.1128/genomeA.00500-14.
65. Mangala Prasad V, Klose T, Rossmann MG. 2017. Assembly, maturation and three-dimensional helical structure of the teratogenic rubella virus. PLoS Pathog 13:e1006377. https://doi.org/10.1371/journal.ppat.1006377.
66. Brien JD, Hassert M, Stone ET, Geerling E, Cruz-Orengo L, Pinto AK. 15 August 2019. Isolation and quantification of Zika virus from multiple organs in a mouse. J Vis Exp https://doi.org/10.3791/59632.
67. Oliphant T, Nybakken GE, Engle M, Xu Q, Nelson CA, Sukupolvi-Petty S, Marri A, Lachmi B-E, Olshevsky U, Fremont DH, Pierson TC, Diamond MS.

2006. Antibody recognition and neutralization determinants on domains I and II of West Nile virus envelope protein. J Virol 80:12149–12159. https://doi.org/10.1128/JVI.01732-06.
68. Baldridge MT, Lee S, Brown JJ, McAllister N, Urbanek K, Dermody TS, Nice TJ, Virgin HW. 2017. Expression of Ifnlr1 on intestinal epithelial cells is critical to the antiviral effects of interferon lambda against norovirus and reovirus. J Virol 91:e02079-16. https://doi.org/10.1128/JVI.02079-16.
69. Schneider CA, Rasband WS, Eliceiri KW. 2012. NIH Image to ImageJ: 25 years of image analysis. Nat Methods 9:671–675. https://doi.org/10.1038/nmeth.2089.
70. Widman DG, Young E, Yount BL, Plante KS, Gallichotte EN, Carbaugh DL, Peck KM, Plante J, Swanstrom J, Heise MT, Lazear HM, Baric RS. 2017. A reverse genetics platform that spans the Zika virus family tree. mBio 8:e02014-16. https://doi.org/10.1128/mBio.02014-16.
71. Deeney S, Powers KN, Crombleholme TM. 2016. A comparison of sexing methods in fetal mice. Lab Anim (NY) 45:380–384. https://doi.org/10.1038/laban.1105.
72. Krikun G, Mor G, Alvero A, Guller S, Schatz F, Sapi E, Rahman M, Caze R, Qumsiyeh M, Lockwood CJ. 2004. A novel immortalized human endometrial stromal cell line with normal progestational response. Endocrinology 145:2291–2296. https://doi.org/10.1210/en.2003-1606.